ACS Catalysis

Letter

Cite This: ACS Catal. 2018, 8, 531−535

pubs.acs.org/acscatalysis

Prism-Shaped Cu Nanocatalysts for Electrochemical CO_2 Reduction to Ethylene

Hyo Sang Jeon,[†] Sebastian Kunze,[†] Fabian Scholten,[†] and Beatriz Roldan Cuenya*[,†,‡,§]

[†]Department of Physics, Ruhr-University Bochum, 44780 Bochum, Germany

[‡]Department of Physics, University of Central Florida, Orlando, Florida 32816, United States

[§]Fritz-Haber-Institut der Max-Planck Gesellschaft, 14195 Berlin, Germany

Supporting Information

ABSTRACT: Electrochemical CO_2 reduction has attracted much attention, because of its advantageous ability to convert CO_2 gas to useful chemicals and fuels. Herein, we have developed prism-shaped Cu catalysts for efficient and stable CO_2 electroreduction by using an electrodeposition method. These Cu prism electrodes were characterized by scanning electron microscopy, X-ray diffraction, and X-ray photoelectron spectroscopy. Electrochemical CO_2 reduction measurements show improved activities for C_2H_4 production with a high partial current density of −11.8 mA/cm^2, which is over four times higher than that of the planar Cu sample (−2.8 mA/cm^2). We have demonstrated that the enhanced C_2H_4 production is partially attributed to the higher density of defect sites available on the roughened Cu prism surface. Furthermore, stability tests show a drastic improvement in maintaining C_2H_4 production over 12 h. The enhanced performance and durability of prism Cu catalysts hold promise for future industrial applications.

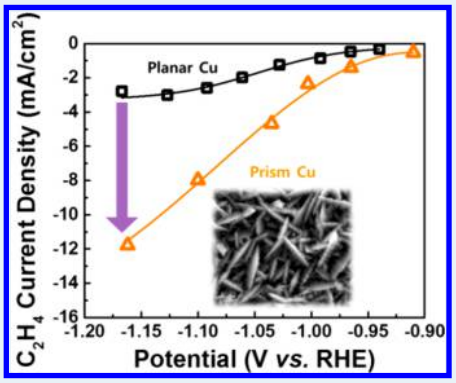

KEYWORDS: *CO_2 reduction, copper, ethylene, shape effects, defects*

The development of sustainable energy sources as an alternative to replace the traditional global energy consumption that is dependent on fossil fuels has recently attracted significant attention, since they are not only being depleted, but causing climate changes due to greenhouse gas CO_2 emission during energy production.[1−3] Electrochemical CO_2 reduction is a promising process to produce useful fuels with high energy density and can be integrated with various renewable energy such as solar and wind in carbon recycling systems, aiming at closing the artificial energy cycle.[4,5] However, CO_2 electroreduction suffers from poor efficiency, because much energy is required to reduce CO_2, which has a thermodynamically stable structure. Therefore, it is critical to develop efficient electrocatalysts for the structure-sensitive CO_2 reduction.

Among the various catalysts for electrochemical CO_2 reduction, copper (Cu) has been identified as the most promising catalyst to produce hydrocarbons such as methane (CH_4) and ethylene (C_2H_4).[6,7] Recently, several researchers have focused on the development of highly selective Cu electrocatalysts for C_2H_4 production, because of their high energy density and their widespread use as chemical feedstock in industry.[8−13] Representatively, Hori et al. reported that single-crystal Cu(100) exhibited high selectivity for C_2H_4 production with a Faradaic efficiency (FE) of ∼40% and an even better result of 50% FE on Cu(711) at −5 mA/cm^2 in 0.1 M $KHCO_3$.[13] However, such single-crystal Cu substrates are not preferred for commercial applications, because of their limitation of scaling up the batch size and high cost. Also, the practical ethylene production rate (i.e., partial current density) of Cu(711) was only −2.5 mA/cm^2, even though it had 50.0% FE of C_2H_4. Therefore, it is important to develop new Cu catalysts with higher production rates for the desired products, such as C_2H_4.

Several studies have suggested that the structure of the Cu surface significantly affects the selectivity of the CO_2 reduction products.[14−20] For example, Chen et al. reported that Cu mesocrystals synthesized by the in situ reduction of a CuCl film were favorable toward C_2H_4 production, where many atomic steps and edges on the Cu mesocrystals surface likely constituted the active sites.[15] Preoxidized and subsequently reduced Cu_2O catalysts have also shown high C_2H_4 product selectivity, which was initially assumed to be due to grain boundaries that are formed during the successive preoxidation and reduction process in the Cu catalysts.[21] The presence of such sites has been proposed to be crucial to enhance the C_2H_4 production, because it helps to improve the adsorption of C1 intermediates required for the C−C bond formation. This hypothesis has been supported by thermal desorption studies revealing that CO molecules are more strongly adsorbed at the surface of preoxidized and subsequently reduced Cu_2O catalysts, compared to polycrystalline Cu.[21]

Received: August 30, 2017
Revised: November 6, 2017
Published: November 29, 2017

DOI: 10.1021/acscatal.7b02959
ACS Catal. 2018, 8, 531−535

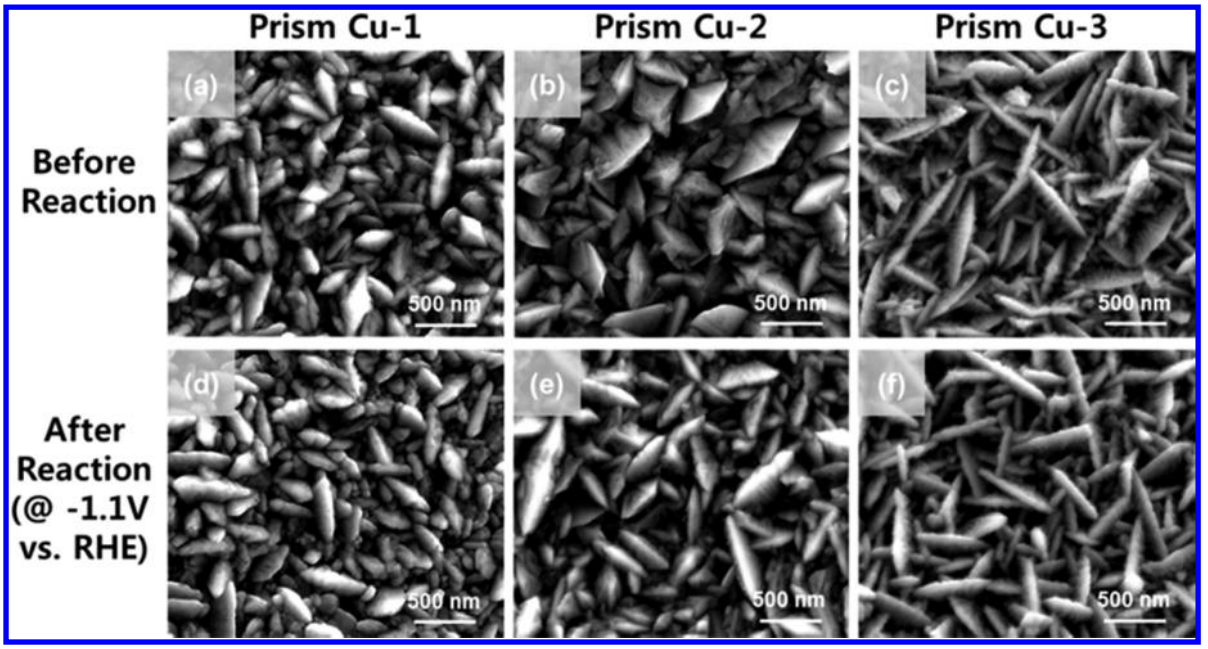

Figure 1. Scanning electron microscopy (SEM) images of prism Cu samples (a–c) before and (d–f) after 2 h of electrochemical CO_2 reduction at −1.1 V vs RHE.

In addition, significant work has been dedicated to the understanding of the various factors affecting the selectivity of the Cu catalysts. The existence of Cu^+ species and subsurface oxygen in preoxidized Cu catalysts under CO_2 electroreduction conditions has been experimentally demonstrated and suggested as an important parameter in the reaction pathway toward C_2H_4 and alcohols.[22] Recent theoretical work was in agreement with the previous experimental work and highlighted how the coexistence of Cu^+/Cu^0 surface species might favor C–C coupling.[23,24] The use of different electrolytes has also been proposed as another crucial factor determining catalyst selectivity.[25−33] For example, the formation of C_2H_4 is favored in an electrolyte with low buffer capacity, such as $KClO_4$ and low concentrated $KHCO_3$, which would produce a high local pH near the electrode surface.[25,26] The activity and selectivity of C_2H_4 formation is also facilitated in the presence of Cs^+ in the bicarbonate solutions,[27,28] as well as in halide-containing electrolytes.[29−31] The nanoparticle size has been reported to also affect the selectivity.[32,33] However, while the majority of studies have focused on investigating the former parameters (i.e., grain boundaries, Cu^+ species, local pH, and size effects, etc.) on CO_2 electroreduction activity and selectivity, much less is known about shape effects, and the role of specific crystalline facets.[34−36]

Herein, we have prepared highly defective prism-shaped Cu catalysts, using a one-step electrodeposition method. Electrochemical CO_2 reduction measurements of prism Cu electrodes have displayed improved activity for C_2H_4 production with stable performance for at least 12 h. We have demonstrated that the presence of a significant fraction of defect sites on the prism Cu surface plays a role in improving C_2H_4 production.

The prism-shaped Cu catalysts were prepared in a Cu^{2+} solution including different concentrations of the additives: 0.4 mM (prism Cu-1), 1.0 mM (prism Cu-2), and 2.0 mM (prism Cu-3). Figures 1a–c, as well as Figure S1 in the Supporting Information, show the surface morphology of the prism Cu-1, prism Cu-2, and prism Cu-3 samples, respectively. All prism Cu samples display perpendicularly grown triangular nanoprisms with different widths of the top and bottom facets, while the planar electropolished Cu reference foil has a flat surface (see Figure S2 in the Supporting Information). In addition, the width of the prisms was more uniform and narrow with increasing additive concentration (Janus Green B) and the side edge surface was found to roughen, leading to a higher concentration of defect sites. Our unique structures of prism Cu are caused by the additive effect acting as a crystal modifier and induces the preferential deposition of Cu ions and the formation of prism-shaped morphologies (see the Supporting Information).

In order to confirm the crystalline structure of the prism Cu, XRD measurements were carried out (see Figure S3 in the Supporting Information). All of the XRD patters were solely associated with the metallic Cu structures (Joint Committee on Powder Diffraction Standards (JCPDS) File No. 04-0836) without other copper oxide phases, such as Cu_2O or CuO. The relative ratio of intensity for (200)/(111) was ∼0.3 for all prism Cu samples, whereas that for planar Cu foil was 0.5 (see Table S1 in the Supporting Information). This result indicated that the growth of prism Cu is preferred along the (111) plane. In addition, the XPS spectra revealed that there were no residual impurities (i.e., N, S, and Cl) from the sample synthesis (Figure S4 in the Supporting Information).

The potential-dependent geometric current densities measured by chronoamperometry were recorded in order to evaluate the electrocatalytic activity of the prism-shaped Cu samples, as shown in Figure 2, as well as Figure S5 in the Supporting Information. We could confirm that prism Cu samples had higher current density than planar Cu within the entire potential region. At a potential of approximately −1.1 V vs RHE, the current densities of planar Cu, prism Cu-1, prism Cu-2, and prism Cu-3 were −10.3, −17.4, −24.7, and −28.6 mA/cm^2, respectively. The three-times-larger current density value of prism Cu-3 can be partially attributed to the higher surface area of the roughened prism Cu (see Figure S6 in the Supporting Information, as well as Table 1). In addition, we could not find any change in the morphology of all catalysts after CO_2 electrolysis at −1.1 V vs RHE for 2 h (Figures 1d–f).

DOI: 10.1021/acscatal.7b02959
ACS Catal. 2018, 8, 531−535

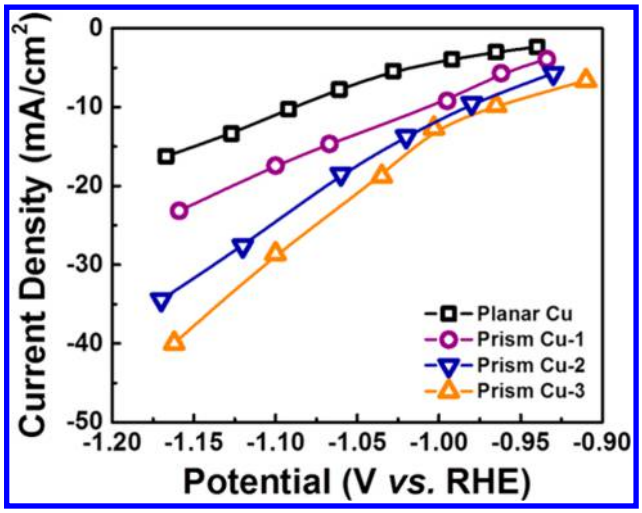

Figure 2. Total geometric current density versus applied potential of a planar Cu foil, prism Cu-1, prism Cu-2, and prism Cu-3.

Table 1. Values of the Electrochemical Double Layer Capacitance and Roughness Factor

sample	capacitance[a] (μF/cm^2)	roughness factor[b]
planar Cu	29	1.0
prism Cu-1	248	8.5
prism Cu-2	365	12.6
prism Cu-3	428	14.8

[a]The double layer capacitances were calculated from the slope of the current density versus the scan rate (Figure S6 in the Supporting Information). [b]The roughness factors were obtained by normalizing the capacitance values by that of the planar Cu sample.

Figure 3, as well as Figure S7 in the Supporting Information, show the partial current densities of gas (i.e., H_2, CO, CH_4, and C_2H_4) and liquid (i.e., HCOOH, C_2H_5OH, and n-C_3H_7OH) products of the CO_2 reduction, as a function of applied potential, and their FE are shown in Figure S8 in the Supporting Information. Although FE has important information in the selectivity of CO_2 reduction products, the partial current density could be helpful to understand the reaction kinetics of the each of the products.[7,37] The partial current density of C_2H_4 of prism Cu-3 was ~11.8 mA/cm^2 at −1.16 V vs RHE. This value was ~4 times higher than that of planar Cu. In contrast to increased C_2H_4 production, we could confirm that the CH_4 partial current density of planar Cu was similar to that of prism Cu samples. This result indicated that the increase in the C_2H_4 production is not simply due to an increase in the surface area of the prism Cu surfaces.

Generally, adsorbed *CO (or CHO*) has been known to be a key intermediate for CH_4 and C_2H_4 formation during CO_2 reduction.[38,39] C_2H_4 is generated by the dimerization of adsorbed *CO in close proximity to each other, followed by hydrogenation, and CH_4 is produced by the hydrogenation of adsorbed *CO. According to the previous reports on polycrystalline Cu for CO_2 reduction, surface-adsorbed C1 intermediates are more favorable to make the CH_4 production at very negative potentials, while C−C bond formation is difficult because the probability of reaction between adjacent C1 intermediates is reduced.[7] Interestingly, the C_2H_4 partial current density of the prism Cu samples dramatically increases with increasing electrolysis potential, while the planar Cu sample displays a constant production rate over −1.1 V vs RHE. This result indicates that the prism Cu samples have certain crystalline facets that favor the dimerization of adsorbed *CO species without a significant change in other factors involved in the hydrogenation of adsorbed *CO.

The prism Cu samples exhibited greater activity for H_2 production than planar Cu, which suggests that the proton that was not participating in the hydrogenation with adsorbed *CO

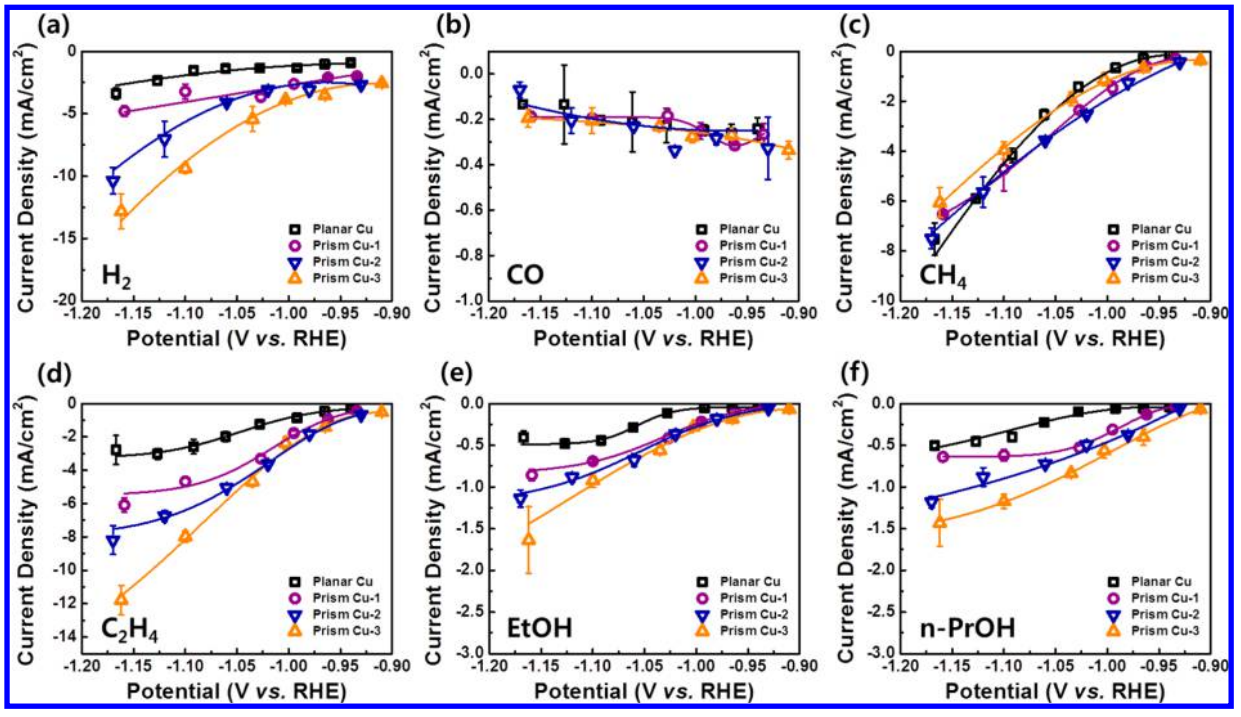

Figure 3. Partial current densities versus applied potential for (a) H_2, (b) CO, (c) CH_4, (d) C_2H_4, (e) ethanol (EtOH), and (f) n-propanol (n-PrOH) of a planar Cu foil, prism Cu-1, prism Cu-2, and prism Cu-3.

DOI: 10.1021/acscatal.7b02959
ACS Catal. 2018, 8, 531−535

to make methane may be released as hydrogen. The CO partial current density of all the samples appears to be the same, which implies that CO, well-known as an intermediate species, was efficiently used to make hydrocarbons. Lastly, we could observe that the C_2H_5OH and n-C_3H_7OH partial current densities increased in the prism Cu samples, which is thought to be related to the improved C_2H_4 formation.[8,40]

We assume that defect sites on the surface of prism Cu samples lead to high C_2H_4 productivity. Tang et al. reported that Cu nanoparticles with roughened surface showed good selectivity toward C_2H_4 formation.[14] They proposed that low-coordination sites on the Cu surface were more likely to enhance C_2H_4 formation, since their DFT calculations indicated that C1 intermediates are more stable at stepped sites on the Cu surface. Recently, Ren et al. showed that Cu nanocrystals exhibited enhanced activity for n-propanol production from CO_2 reduction, because numerous defect sites on their surfaces stabilized the C_2H_4 intermediates.[40] In particular, through simple cyclic voltammetry (CV) measurement, they identified the voltammetric feature for the defect sites by confirming unique reduction peaks on their Cu nanocrystal catalysts, which are absent in Cu single-crystal surfaces. Interestingly, they found that the integrated charge values of this peak (i.e., proportional to the number of defect sites) correlated linearly to the production rate of n-propanol.[40] Our CV experiments also served to identify the density of the defect sites on the prism Cu samples. We found reduction peaks at the potential region between −0.25 and 0 V vs RHE, which are in good agreement with previous results (see Figure 4, as well as Figure S9 in the Supporting Information).[40] A

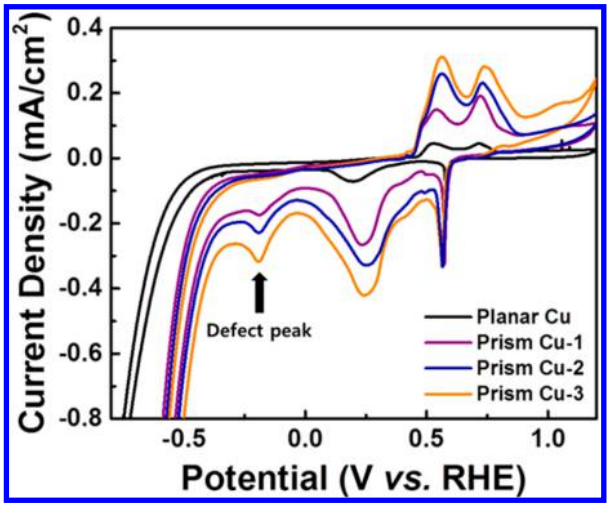

Figure 4. Cyclic voltammograms of a planar Cu foil, prism Cu-1, prism Cu-2, and prism Cu-3 in N_2-saturated 0.1 M $KHCO_3$ electrolyte.

relatively intense reduction peak was observed in the Cu prism samples, while planar Cu showed weak peak intensity at the same potential region. This result indicates that C_2H_4 production of our prism Cu samples is improved by the numerous defects sites on the prism Cu surfaces.

However, even though strong defect-related peaks were observed in our voltammograms, we could not find a direct correlation when comparing the C_2H_4 partial current density and the integrated charge values of the defect peak. Therefore, there should be other factors that are also involved in the increased C_2H_4 production of prism Cu. One factor that might contribute to the observed enhanced C_2H_4 selectivity would be the possible existence of Cu^+ species in the catalysts under CO_2 reduction reaction conditions, which was observed in preoxidized Cu catalysts and assigned to favor C−C coupling.[23,24] To prove the chemical state of prism Cu catalysts during the CO_2 reduction reaction, quasi-in situ X-ray photoelectron spectroscopy (XPS) measurements were carried out. The prism Cu-3 sample was measured via XPS before and after 2 h of CO_2 electroreduction at −1.1 V vs RHE. The Cu Auger LMM spectra shown in Figure S10 in the Supporting Information indicate that the prism Cu-3 sample contained metallic Cu and Cu oxide species before the reaction, formed upon sample exposure to air. However, after the reaction, no Cu^+ species were detected. This result indicates that the oxidation state of our Cu prism catalysts does not play a role in the observed ethylene selectivity.

Another possible factor is a modification of the local pH, since it has been reported that the reaction pathway of CO_2 reduction is preferred toward C_2H_4 formation when the local pH increases.[28,41] Thus, it is expected that the increase of the local pH due to high current densities on the highly roughened prism Cu surface could lead to a reaction pathway toward C_2H_4 formation. As a result, the enhanced C_2H_4 production of the prism Cu samples is postulated to be due to the simultaneous effect of local pH changes and the presence of defect sites.

Lastly, the stability of the prism Cu-3 was investigated at −1.1 V vs RHE for 12 h (Figure 5). In our setup, a Selemion

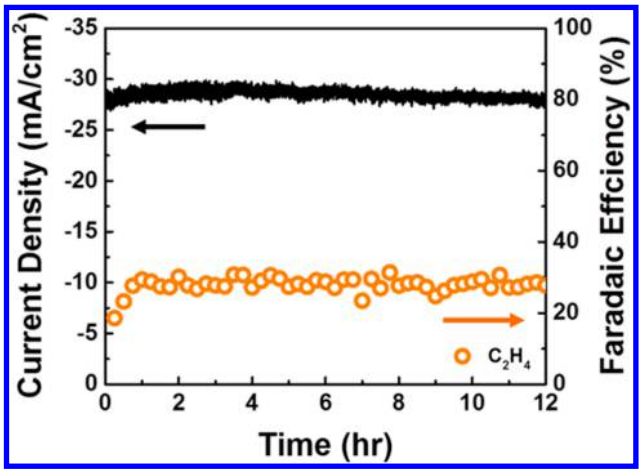

Figure 5. Total current density and C_2H_4 FE of prism Cu-3 at −1.1 V vs RHE for 12 h.

membrane was installed to separate the cathode and anode parts and 0.1 M $KHCO_3$ electrolyte was used after purifying the trace metal ion impurities by using a cation-exchange resin (i.e., Chelex 100 resin).[42,43] The total current density and C_2H_4 FE were maintained at an almost constant level of ∼28.6 mA cm^{-2} and ∼27.8%, respectively, which means that C_2H_4 gas is consistently produced at a rate of ∼24.7 μmol h^{-1} cm^{-2} on our prism Cu electrodes. Interestingly, when we conducted the same stability measurement in the unpurified electrolyte, we could confirm that the C_2H_4 FE dramatically decreased while the H_2 FE increased (Figure S11 in the Supporting Information). This is explained by the previous research conducted by Wuttig et al., demonstrating that trace amounts of metal impurities in the electrolyte were simultaneously deposited on the electrode surface during the CO_2 reduction reaction, which resulted in an increase in the H_2 evolution reaction over time while suppressing the CO_2 reduction reaction.[42] Being able to remove such metal impurities, as was implemented here, is of major importance in order to

DOI: 10.1021/acscatal.7b02959
ACS Catal. 2018, 8, 531−535

achieve a prolonged stability during CO_2 reduction reactions. Our prisms Cu appear to be promising catalyst candidates, because of their simple synthesis, high performance, and durability.

In summary, we have prepared prism-shaped Cu electrocatalysts via an electrochemical deposition method, using a crystal modifier additive. The prism Cu samples exhibited high CO_2 reduction reaction activity, in terms of C_2H_4 production, and excellent stability over at least 12 h. It is expected that the enhanced C_2H_4 production is attributed to the simultaneous effect of possible changes in the local pH and the presence of low-coordinated atoms at defect sites on the roughened Cu prism surface.

■ ASSOCIATED CONTENT

Supporting Information

The Supporting Information is available free of charge on the ACS Publications website at DOI: 10.1021/acscatal.7b02959.

Experimental details, additional SEM images, XRD data, XPS data, Faradaic efficiency, and additional analysis of the electrochemical data (PDF)

■ AUTHOR INFORMATION

Corresponding Author

*E-mail: Roldan@fhi-berlin.mpg.de.

ORCID

Beatriz Roldan Cuenya: 0000-0002-8025-307X

Notes

The authors declare no competing financial interest.

■ ACKNOWLEDGMENTS

This work was funded by the German Federal Ministry of Education and Research (BMBF) under Grant Nos. 03SF0523C (CO2EKAT) and 033RCOO4D (eEthylene), the Cluster of Excellence RESOLV at RUB (No. EXC 1069) funded by the Deutsche Forschungsgemeinschaft, and the ERC OPERANDO-CAT (No. ERC-725915). In addition, financial support was provided by the U.S. National Science Foundation (No. NSF-CHEM 1213182). The authors acknowledge Xingli Wang (TU Berlin) and Dr. Fernando Rinaldi (Bruker AXS GmbH) for XRD measurements.

■ REFERENCES

(1) Turner, J. A. *Science* **1999**, *285*, 687−689.
(2) Centi, G.; Quadrelli, E. A.; Perathoner, S. *Energy Environ. Sci.* **2013**, *6*, 1711−1731.
(3) Lewis, N. S.; Nocera, D. G. *Proc. Natl. Acad. Sci. U. S. A.* **2006**, *103*, 15729−15735.
(4) Whipple, D. T.; Kenis, P. J. A. *J. Phys. Chem. Lett.* **2010**, *1*, 3451−3458.
(5) Kondratenko, E. V.; Mul, G.; Baltrusaitis, J.; Larrazabal, G. O.; Pérez-Ramírez, J. *Energy Environ. Sci.* **2013**, *6*, 3112−3135.
(6) Hori, Y. In *Modern Aspects of Electrochemistry*, Vol. *42*; Vayenas, C. G., White, R. E., Gamboa-Aldeco, M. E., Eds.; Springer: New York, 2008.
(7) Kuhl, K. P.; Cave, E. R.; Abram, D. N.; Jaramillo, T. F. *Energy Environ. Sci.* **2012**, *5*, 7050−7059.
(8) Ren, D.; Deng, Y.; Handoko, A. D.; Chen, C. S.; Malkhandi, S.; Yeo, B. S. *ACS Catal.* **2015**, *5*, 2814−2821.
(9) Yano, H.; Tanaka, T.; Nakayama, M.; Ogura, K. *J. Electroanal. Chem.* **2004**, *565*, 287−293.
(10) Reller, C.; Krause, R.; Volkova, E.; Schmid, B.; Neubauer, S.; Rucki, A.; Schuster, M.; Schmid, G. *Adv. Energy Mater.* **2017**, *7*, 1602114.
(11) Handoko, A. D.; Ong, C. W.; Huang, Y.; Lee, Z. G.; Lin, L.; Panetti, G. B.; Yeo, B. S. *J. Phys. Chem. C* **2016**, *120*, 20058−20067.
(12) Engelbrecht, A.; Hämmerle, M.; Moos, R.; Fleischer, M.; Schmid, G. *Electrochim. Acta* **2017**, *224*, 642−648.
(13) Hori, Y.; Takahashi, I.; Koga, O.; Hoshi, N. *J. Mol. Catal. A: Chem.* **2003**, *199*, 39−47.
(14) Tang, W.; Peterson, A. A.; Varela, A. S.; Jovanov, Z. P.; Bech, L.; Durand, W. J.; Dahl, S.; Norskov, J. K.; Chorkendorff, I. *Phys. Chem. Chem. Phys.* **2012**, *14*, 76−81.
(15) Chen, C. S.; Handoko, A. D.; Wan, J. H.; Ma, L.; Ren, D.; Yeo, B. S. *Catal. Sci. Technol.* **2015**, *5*, 161−168.
(16) Mistry, H.; Varela, A. S.; Kühl, S.; Strasser, P.; Roldan Cuenya, B. *Nat. Rev. Mater.* **2016**, *1*, 16009.
(17) Yang, K. D.; Ko, W. R.; Lee, J. H.; Kim, S. J.; Lee, H.; Lee, M. H.; Nam, K. T. *Angew. Chem., Int. Ed.* **2017**, *56*, 796−800.
(18) Lee, S.; Kim, D.; Lee, J. *Angew. Chem., Int. Ed.* **2015**, *54*, 14701−14705.
(19) Sen, S.; Liu, D.; Palmore, G. T. R. *ACS Catal.* **2014**, *4*, 3091−3095.
(20) Li, C. W.; Kanan, M. W. *J. Am. Chem. Soc.* **2012**, *134*, 7231−7234.
(21) Verdaguer-Casadevall, A.; Li, C. W.; Johansson, T. P.; Scott, S. B.; McKeown, J. T.; Kumar, M.; Stephens, I. E. L.; Kanan, M. W.; Chorkendorff, I. *J. Am. Chem. Soc.* **2015**, *137*, 9808−9811.
(22) Mistry, H.; Varela, A. S.; Bonifacio, C. S.; Zegkinoglou, I.; Sinev, I.; Choi, Y.-W.; Kisslinger, K.; Stach, E. A.; Yang, J. C.; Strasser, P.; Roldan Cuenya, B. *Nat. Commun.* **2016**, *7*, 12123.
(23) Favaro, M.; Xiao, H.; Cheng, T.; Goddard, W. A.; Yano, J.; Crumlin, E. J. *Proc. Natl. Acad. Sci. U. S. A.* **2017**, *114*, 6706−6711.
(24) Cheng, T.; Xiao, H.; Goddard, W. A. J. *Proc. Natl. Acad. Sci. U. S. A.* **2017**, *114*, 1795−1800.
(25) Ma, M.; Djanashvili, K.; Smith, W. A. *Angew. Chem.* **2016**, *128*, 6792−6796.
(26) Schouten, K. J. P.; Pérez Gallent, E.; Koper, M. T. M. *J. Electroanal. Chem.* **2014**, *716*, 53−57.
(27) Murata, A.; Hori, Y. B. *Bull. Chem. Soc. Jpn.* **1991**, *64*, 123−127.
(28) Singh, M. R.; Kwon, Y.; Lum, Y.; Ager, J. W.; Bell, A. T. *J. Am. Chem. Soc.* **2016**, *138*, 13006−13012.
(29) Varela, A. S.; Ju, W.; Reier, T.; Strasser, P. *ACS Catal.* **2016**, *6*, 2136−2144.
(30) Ogura, K.; Ferrell, J. R.; Cugini, A. V.; Smotkin, E. S.; Salazar-Villalpando, M. D. *Electrochim. Acta* **2010**, *56*, 381−386.
(31) Gao, D.; Scholten, F.; Roldan Cuenya, B. *ACS Catal.* **2017**, *7*, 5112−5120.
(32) Reske, R.; Mistry, H.; Behafarid, F.; Roldan Cuenya, B.; Strasser, P. *J. Am. Chem. Soc.* **2014**, *136*, 6978−6986.
(33) Mistry, H.; Reske, R.; Zeng, Z.; Zhao, Z.; Greeley, J.; Strasser, P.; Roldan Cuenya, B. *J. Am. Chem. Soc.* **2014**, *136*, 16473−16476.
(34) Loiudice, A.; Lobaccaro, P.; Kamali, E. A.; Thao, T.; Huang, B. H.; Ager, J. W.; Buonsanti, R. *Angew. Chem., Int. Ed.* **2016**, *55*, 5789−5792.
(35) Roberts, F. S.; Kuhl, K. P.; Nilsson, A. *Angew. Chem.* **2015**, *127*, 5268−5271.
(36) Gao, D.; Zegkinoglou, I.; Divins, N. J.; Scholten, F.; Sinev, I.; Grosse, P.; Roldan Cuenya, B. *ACS Nano* **2017**, *11*, 4825−4831.
(37) Martin, A. J.; Larrazabal, G. O.; Pérez-Ramírez, J. *Green Chem.* **2015**, *17*, 5114−5130.
(38) Schouten, K. J. P.; Kwon, Y.; van der Ham, C. J. M.; Qin, Z.; Koper, M. T. M. *Chem. Sci.* **2011**, *2*, 1902−1909.
(39) Peterson, A. A.; Abild-Pedersen, F.; Studt, F.; Rossmeisl, J.; Norskov, J. K. *Energy Environ. Sci.* **2010**, *3*, 1311−1315.
(40) Ren, D.; Wong, N. T.; Handoko, A. D.; Huang, Y.; Yeo, B. S. *J. Phys. Chem. Lett.* **2016**, *7*, 20−24.
(41) Kas, R.; Kortlever, R.; Yılmaz, H.; Koper, M. T. M.; Mul, G. *ChemElectroChem* **2015**, *2*, 354−358.
(42) Wuttig, A.; Surendranath, Y. *ACS Catal.* **2015**, *5*, 4479−4484.
(43) Hall, A. S.; Yoon, Y.; Wuttig, A.; Surendranath, Y. *J. Am. Chem. Soc.* **2015**, *137*, 14834−14837.

DOI: 10.1021/acscatal.7b02959
ACS Catal. 2018, 8, 531−535